Hypercholesterolemia aggravates in-stent restenosis in rabbits: a mitigating effect of stent surface modification with CD47-derived peptide.

Ilia Fishbein*, Vaishali V Inamdar*, Ivan S Alferiev, George Bratinov, Menekhem M. Zviman, Anna Yekhilevsky, Chandrasekaran Nagaswami, Kristin L. Gardiner, Robert J Levy, Stanley J Stachelek

Abstract:

Background: Hypercholesterolemia (HC) has previously been shown to augment restenotic response in several animal models and humans. However, the mechanistic aspects of in-stent restenosis (ISR) on a hypercholesterolemic background, including potential augmentation of systemic and local inflammation precipitated by HC are not completely understood. CD47 is a transmembrane protein known to abort crucial inflammatory pathways. Our present studies have examined the interrelation between HC, inflammation, and ISR and investigated the therapeutic potential of stents coated with a CD47-derived peptide (pepCD47) in the hypercholesterolemic rabbit model.

Methods and Results: PepCD47 was immobilized on metal foil coupons and stents using polybisphosphonate coordination chemistry and pyridyldithio/thiol conjugation. The relative abundance of the surface-associated cells on bare metal (BM) and pepCD47 foils exposed to whole rabbit blood showed a 40% inhibition of cell attachment on pepCD47-modified surfaces. Likewise, M1 cytokine expression analyzed in buffy coat-derived cells cultured over the BM and pepCD47-derivatized foils demonstrated a>80% decrease in TNFa and MCP1 levels with the pepCD47 coating. Rabbits with diet-induced hypercholesterolemia and normocholesterolemic counterparts underwent bilateral implantation of BM and pepCD47 stents in the iliac location. Hypercholesterolemia increased neointimal area and percent of luminal stenosis in comparison with normocholesterolemic animals at 4 weeks post-stenting (2.07±0.52 vs 0.64±0.15 mm^2 and 54.32±13.01 vs 23.30±4.36%, respectively). These untoward outcomes were mitigated (54% and 50% for neointimal area and percent of luminal stenosis) in the arteries of hypercholesterolemic rabbits treated with pepCD47-derivatized stents. Compared to NC animals, TNFa immunopositivity and MΦ infiltration of peri-strut areas increased in HC group animals 1.81- and 2.58-fold, respectively, and was attenuated in the arteries of hypercholesterolemic rabbits treated with pepCD47 stents.

Conclusions: Augmented inflammatory responses triggered by HC underlie severe ISR morphology in hypercholesterolemic rabbits. Blockage of initial platelet and leukocyte

attachment to stent struts through CD47 functionalization of stents mitigates pro-restenotic effects of HC.

Introduction

Development of ISR in stented atherosclerotic coronary and peripheral arteries is a common complication of stent angioplasty[1]. Even in the era of advanced drug-eluting stents (DES), ISR complicates up to 10% of the coronary interventions[2], with the numbers being even higher for patients with certain comorbidities[3]. Given the decisive role of dyslipidemia in the progression of atherosclerosis, the significance of hypercholesterolemia for ISR pathogenesis has been scrutinized for a long time, yet the clinical data are controversial[4-6]. The most plausible link between the elevated total and the low-density lipoprotein-associated cholesterol (LDL-C) and ISR is increased systemic and vascular inflammation associated with hypercholesterolemia[7, 8]. Increased uptake of cholesterol by endothelial cells promotes monocyte attachment and transmigration into the subendothelial space via upregulated expression of cell adhesion molecules[9, 10]. Monocytes differentiate into macrophages and produce multiple cytokines that, by paracrine action, amplify the initial damage to healthy endothelium triggered by hypercholesterolemia[11]. Furthermore, the compensatory anti-inflammatory mechanisms mediated by nitric oxide (NO) get depressed because of reduced NO production by the dysfunctional endothelium and its decreased bioavailability due to NO sequestration by reactive oxygen species[12]. In addition, hypercholesterolemic states induce thrombocythemia and activate platelets to adhere to activated endothelium priming it for neutrophil and monocyte ingress[13, 14]. CD47 is a "marker of self" ubiquitously expressed on the cell surface to protect the host from the attack by its own immune system[15, 16]. We have previously shown that CD47[17, 18], and CD47-derived peptides[19, 20] bestow protection from platelet and inflammatory cell attachment to the surface of biomaterials. We also demonstrated that the stainless-steel surfaces of stents functionalized with a 22-aminoacid peptide derived from the extracellular Ig domain of rat CD47 are partially protected from platelet and leukocyte association and reduce ISR after carotid artery implantation in a rat model of stent angioplasty[20]. Since this study used healthy normocholesterolemic rats, the results do not entirely reflect the complex relationship between hypercholesterolemia, vascular and systemic inflammation, and the therapeutic effectiveness of CD47-modified stents. The current study aimed to elaborate on the role of inflammation as a link between hypercholesterolemia and the exacerbated response to vascular injury and to

study the anti-inflammatory and anti-restenotic effects of CD47-derivatized stents in a clinically relevant animal model.

Materials and Methods

Materials, chemicals, and biologicals.

316-grade stainless steel foils and tubes were from Goodfellow (Coraopolis, PA, USA) and Microgroup (Medway, MA, USA), respectively. Open cell design stainless steel (316L) stents were obtained from C2D Medical (Ahmedabad, India). Tris (2-carboxyethyl) phosphine hydrochloride (TCEP·HCl) and Vybrant ™ CFDA SE Cell Tracer Kit were purchased from Thermo Fisher Scientific (Waltham, MA, USA). 4 % glutaraldehyde and 0.1M Sodium Cacodylate buffer pH 7.4 were obtained from Electron Microscopy Sciences (Hatfield, PA). A peptide derived from the extracellular Ig domain of rabbit CD47 (Ac-Gly-Asn-Tyr-ThrCys-Glu-Val-Thr-Glu-Leu-Ser-Arg-Glu-Gly-Lys-Thr-Val-Ile-Glu-Leu-Lys-LINKER-Cys-OH) was custom synthesized by Bachem (Torrance, CA, USA). A terminal reactive cysteine residue was attached to the pepCD47 core sequence through a dual hydrophilic spacer (AEEAc-AEEAc). Polyallylamine bisphosphonate with latent thiol groups (PABT) and polyethylenimine with installed pyridyldithio groups (PEI-PDT) were synthesized in our lab according to the published procedures (REF). All other chemicals were from Sigma-Aldrich. All cell culture reagents were from Thermo Fisher Scientific (Waltham, MA, USA). A cholesterol fluorimetric assay kit was purchased from Cayman Chemicals (Ann Arbor, MI, USA). ELISA kits for rabbit TNFα and IL1β were from G-biosciences (St. Louis, MO, USA). A lipid peroxidase assay kit was from Eagle Biosciences (Amherst, NH, USA). Elastic tissue Verhoeff-van Gieson staining kit was obtained from Sigma-Aldrich (St-Louis, MO, USA). Primary antibodies to rabbit CD68, TNFα, IL1β, and IL6 were from ProSci (Poway, CA, USA), MyBioSource (San Diego, CAS, USA), Bioss (Woburn, MA, USA), and Abbexa (Cambridge, UK), respectively.

pepCD47 functionalization of stainless steel.

Metal samples were washed in isopropanol and chloroform at 55□C to remove impurities and baked in an air atmosphere at 220□C for 30 min. The specimens were then reacted with 0.5% aqueous solution of PABT at 60□C with shaking for 2 hours, followed by washing in DDW and exposure to 10 mg/ml TCEP·HCl in 0.1M acetic buffer at 28□C for 10 min to deprotect thiols. The samples were then washed with degassed DDW and reacted in an argon atmosphere with a degassed 1% aqueous solution of PEI-PDT at 37□C for 40 min and thoroughly washed with DDW. Rabbit CD47-derived peptide (0.5 mg in 1 ml of 50% trichloroacetic acid) bearing free

thiols was further diluted with degassed dimethylformamide/PBS mixture and reacted in argon atmosphere with thiol-reactive PDT groups on the surface of metal samples at 37□C with shaking for 30 min. The metal specimens were then washed in sterile PBS and stored at 4□C prior to use.

Chandler loop experiments.

PepCD47 surface-modified or unmodified stainless steel tube inserts (10 mm length, 6.3 mm diameter) were placed in succession with 1 cm intervals into the 40-cm sections of 1/4" PVC tubing (Terumo Cardiovascular Systems, Ann Arbor, MI). Ten ml of NC and HC rabbit blood anticoagulated with sodium citrate (0.6% final concentration) was perfused through the tubing for 3 hours at a shear rate of 20 dyn/cm^2. At the end of the perfusion period, the steel inserts were removed, gently washed with PBS, and processed, determining cell and platelet adhesion to the metal substrate by CFDA staining and SEM, as detailed below.

CFDA staining. To visualize the platelets and inflammatory leukocytes attached to the adluminal surface of the inserts, non-fixed specimens were exposed to 10 μM Vybrant ™ CFDA SE at 37^{0}C for 15 mins. The samples were then thoroughly washed with PBS and fixed in 4% paraformaldehyde at room temperature for 1 hour. The tubes were then cut longwise, inverted, and imaged using a fluorescence microscope (Nikon TE300). The samples were also analyzed fluorimetrically (ex 485 nm, em 538 nm, cut-off 530 nm) using Spectra Max Gemini EM (Molecular Devices, Sunnyvale, CA).

Scanning electron microscopy. After removing from the Chandler loop apparatus, pepCD47-functionalized and non-modified stainless-steel inserts exposed to HC blood were gently washed with PBS and fixed in 2% glutaraldehyde in sodium cacodylate buffer with 0.1M sodium chloride for 24 hours. The inserts were then cut longwise, inverted, rinsed with DDW, dehydrated serially with 70-100% ethanol and hexamethyldisilazane, and sputter-coated with gold palladium. Ten digital micrographs (magnification range 500-10000) at random areas were acquired for analysis using SEM (Quanta250, FEI, Hillsboro, OR). Platelet and leukocyte attachment in 4 random fields was determined by manual counting.

Macrophage polarization on the pepCD47-modified and non-modified metal substrate (PCR studies).

Platelet-depleted buffy coats from NC and HC rabbit blood were seeded in the wells of a 12-well plate containing 15 mm x 15 mm stainless steel foil coupons, either non-modified or pepCD47-functionalized (n=4 for each group). The medium was changed after 4 hours for complete

RPMI-1640 supplemented with 100 ng/ml of human MCSF that was shown to support the growth and differentiation of rabbit macrophages (REF). The medium was changed every other day. After 6 days of the culture, cells growing on the cell culture plastic (control) and those growing on the different steel substrates were lysed. RNA was isolated using an RNeasy kit (Qiagen, Germantown, MD, USA) and reverse transcribed in cDNA with TaqMan reverse transcription reagents (Applied Biosystems, Waltham, MA, USA). cDNA was amplified in RT-PCR reaction with Sybr Green and rabbit inflammatory cytokine primers (IDT, Coralville, IA, USA), reflecting the M1 and M2 polarization phenotypes.

In vivo studies.

All animal experiments were pre-approved by the University of Pennsylvania IACUC and conformed to all relevant regulations. Some animals were fed an HC diet (a standard rabbit chow supplemented with 1% cholesterol and 3% peanut oil) (Bioserv, Flemington, NJ, USA). Blood for monocyte isolation was harvested from the central ear artery. For stent surgery, in isoflurane-anesthetized rabbits of either gender (3-4 kg) vascular access was surgically obtained with arteriotomy in the right carotid artery. Under fluoroscopic control, a 4-Fr sheath was advanced over the 0.035" guidewire to the distal aorta. The guidewire was exchanged for a 0.014" guide wire, over which a 3-Fr Fogarty catheter was inserted in the left common iliac artery. A balloon of the Fogarty catheter was inflated and passed across the artery three times to denude the endothelium, after which the Fogarty catheter was exchanged for a 3.0 mm angioplasty catheter loaded with a stent. The stent was deployed in the segment of the iliac artery devoid of the side branches at 12-14 atm to achieve a stent/artery diameter ratio of 1.3. The guidewire was then relocated into the right common iliac artery, and the sequence of Fogarty balloon denudation/stent deployment was repeated. In the NC rabbits, both stents were BMS, while in the HC rabbit group, one of the stents was BMS, and the other was a pepCD47 stent. All animals were euthanized 28 days after stent placement.

Results

To study the attachment of bloodborne cells to the native and pepCD47-modified metal substrate, the relative number of cells adhered to the stainless-steel samples was quantified using CFDA staining and fluorimetry after 3-hour exposure to NC and HC rabbit blood recirculated in a Chandler loop apparatus. While no significant differences between the non-modified and pepCD47-modified samples was noted with NC blood (Fig. 1 A, B, and E), the

number of cells on the metal surface exposed to HC blood was reduced by 35% as a result of CD47 functionalization (Fig. 1 C, D and E). These results were further confirmed by scanning electron microscopy that demonstrated a 3.2-fold decrease in the number of platelets from HC blood deposited on CD47-modified steel surface (Fig. 1 F-H). The presence of pepCD47 fostered M2 polarization of the macrophages derived from the buffy coats that originated from NC and HC rabbit blood as evidenced by increased M2/M1 cytokine gene expression ratio in macrophages cultured on the bare metal and CD47-functionalized surfaces (Fig 2). The expression of signature M1 cytokines, IL1b and IL12, was suppressed in macrophages growing on the CD47-modified surface compared to macrophages cultured on bare metal steel (Fig. 2 A and B). In contrast, the M2 cytokines, IL10 and TGFb demonstrated opposite kinetics (Fig. 2 C and D).

To investigate the impact of hypercholesterolemia on ISR development and the antirestenotic effectiveness of CD47 stent functionalization, BMS and stents modified with pepCD47 were implanted in rabbits fed normal chow and HC diet. Exposure to a hypercholesterolemic diet (4 weeks before the intervention and 4 weeks after stent deployment) considerably increased neointimal formation in the stented iliac arteries (Fig. 3 A and B). Neointimal area (Fig. 3 D), neointimal thickness (Fig. 3 E), percent of luminal stenosis (Fig. 3 F), and neointima-to-media ratio (Fig. 3 G) increased 2.3-5.2 fold in the hypercholesterolemic animals. These hyperplastic responses to stent implantation were reversed 29-52% ($p<0.01$ for all comparisons) in the arteries treated with the pepCD47-derivatized stents (Fig. 3 A-G).

In the individual animals treated with BMS, the severity of ISR expressed as neointima to media ratio strongly correlated (Pearson coefficient of 0.826; $p<0.0001$) with total cholesterol levels in rabbit blood (Fig. 4). BMS implantation in hypercholesterolemic animals was associated with increased plasma concentrations of inflammatory markers, TNFα (Fig. 5 A) and IL1β (Fig. 5 B), and lipid peroxidation marker, malondialdehyde (Fig. 5 C) compared to normocholesterolemic rabbits. Likewise, local arterial expression of inflammatory markers, TNFα (Fig. 6 A, B, and D), IL1β (Fig. 6 E, F, and H), and IL6 (Fig. 6 I, J, and L) was significantly upregulated in the peri-strut regions of hypercholesterolemic rabbits compared to normocholesterolemic counterparts. Furthermore, inflammatory macrophage infiltrates were significantly more predominant in the peri-strut regions of hypercholesterolemic rabbits as compared to normocholesterolemic animals (Fig. 6 M, N, and P). Local expression of inflammatory markers and the presence of macrophages around the struts was significantly reduced in the arteries of hypercholesterolemic

animals treated with pepCD47-functionalized stents (compare Fig. 6 B and C, F and H, J and K, N and O). Macrophages accumulating in the peri-strut location appear to present the principal source of proinflammatory cytokines, as apparent from dual immunofluorescence staining of macrophages and IL1β-producing cells (Fig. 7). Activation of quiescent cells of the vascular wall by the macrophage-released cytokines drives and sustains cell proliferation, migration, and ECM production, thus contributing to the neointimal formation and ISR. In BMS-treated hypercholesterolemic animals, proliferation in the neointimal, medial, and adventitial compartments increased compared to normocholesterolemic counterparts (Fig. 8 A, B, and D) and was significantly reduced in the arteries treated with pepCD47-modified stents (Fig. 8 B, C and D).

Figure Legends

Fig. 1 Blood interaction with pepCD47-modified and non-modified stainless steel surface in the Chandler loop flow experiments.

(A-D) Fluorescence microscopy images (FITC filter set; original magnification - 200x) of adluminal surface of non-modified (A, B) and pepCD47-modified (C, D) stainless steel inserts exposed to NC (A, C) or HC (B, D) rabbit blood recirculating in the Chandler loop apparatus (n=4 per sample type, blood type). E. Fluorimetry measurement of the relative fluorescence emitted by CFDA SE stained cells associated with the adluminal surface. (F-G) Scanning electron microscopy images (original magnification – 500x; insets – 5,000x) of the adluminal surface of non-modified (F) and pepCD47-modified (G) stainless steel inserts exposed to HC rabbit blood recirculating in the Chandler loop apparatus (n=3 per sample type). (H) The surface density of attached platelets.

Fig. 2 Relative expression of M1 (IL1β and IL12) and M2 (IL10 and TGFβ) macrophage polarization markers by macrophages growing on the bare metal and pepCD47-modified surface.

(A-D) Relative quantification (RQ) by $2^{-\delta\delta ct}$ method of IL1β (A), IL12 (B), IL10 (C) and TGFβ (D) expression by rabbit NC and HC blood-derived macrophages grown on the cell culture plastic (control), bare metal surface (BMS) and pepCD47-modified steel (n=3 per condition).

Fig. 3 Effects of hypercholesterolemia and stent surface functionalization with pepCD47 on the extent of ISR.

(A-C) Representative microscopy images of stented iliac arteries of NC (A) and HC (B, C) rabbits treated with bare metal (A, B) and pepCD47 stents (original magnification is 20x). Stent struts were removed by acid treatment(REF) prior to paraffin embedding, sectioning and Verhoef-van Gieson staining. n – neointima, m – media, a – adventitia, l – lumen, s – strut positions. (D-G) Morphometric values of neointimal area (D), neointima thickness above the struts (E), percent of luminal stenosis (F), and neointima to media area ratio in the treatment groups.

Fig. 4 A correlation between the individual plasma cholesterol concentrations and the severity of ISR.

Individual levels of plasma cholesterol at euthanasia and the respective N/M ratio values are plotted.

Fig. 5 Plasma concentrations of inflammatory and oxidative stress markers in NC and HC rabbits.

(A-C) Concentrations of TNFα (A), IL1β (B), and malondialdehyde (C) as determined by ELISA in plasma of NC (n=5) and HC (n=5) rabbits.

Fig. 6 Immunohistochemical assessment of the inflammatory cytokine expression in the peri-strut areas of NC and HC rabbits implanted bare metal and pepCD47-modified stents.

(A-P) Representative microscopic images (100x magnification) of iliac arteries stented with BMS (A, B, E, F, I, J, M, N) and pepCD47-functionalized stents (C, G, K, O) and immunostained for TNFα (A-C), IL1β (E-G), IL6 (I-K) and CD68-positive macrophages (M-O). Quantification of TNFα (D), IL1β (H), and IL6 (L) expression was based on a semi-quantitative (0-4) scale. Macrophage infiltration around the struts (P) was calculated as a percentage of a strut circumference occupied with the CD68-positive cells (n=4 for each marker/treatment group combination).

Fig. 7 Co-localization of inflammatory cytokine-producing cells with macrophages.

(A-C) Microscopic images (original magnification – 200x) of stented arterial section co-stained with anti-CD68 (A) and anti-IL1β (B) antibodies. Merged image (C) demonstrates spatial co-localization of CD68 and IL1β expression.

Fig. 8 Cell proliferation in the stented arteries.

(A-C) Ki67 immunohistochemistry was performed on the sections from the stented iliac arteries of NC (A) and HC (B, C) rabbits treated with BMS (A, B) and pepCD47-modified stents (C). Ki67 labeling was expressed as the number of Ki67-positive cells per mm^2 of neointimal, medial, and adventitial compartments (D).

1. Alfonso F, Byrne RA, Rivero F and Kastrati A. Current treatment of in-stent restenosis. *J Am Coll Cardiol*. 2014;63:2659-73.
2. Moussa ID, Mohananey D, Saucedo J, Stone GW, Yeh RW, Kennedy KF, Waksman R, Teirstein P, Moses JW and Simonton C. Trends and Outcomes of Restenosis After Coronary Stent Implantation in the United States. *J Am Coll Cardiol*. 2020;76:1521-1531.
3. Rathore S, Terashima M, Katoh O, Matsuo H, Tanaka N, Kinoshita Y, Kimura M, Tuschikane E, Nasu K, Ehara M, Asakura K, Asakura Y and Suzuki T. Predictors of angiographic restenosis after drug eluting stents in the coronary arteries: contemporary practice in real world patients. *EuroIntervention*. 2009;5:349-54.
4. Lerakis S, El-Chami MF, Patel AD, Veledar E, Alexopoulos E, Zacharoulis A and Triantafyllou A. Effect of lipid levels and lipid-lowering therapy on restenosis after coronary artery stenting. *Am J Med Sci*. 2006;331:270-3.
5. Sud M, Han L, Koh M, Abdel-Qadir H, Austin PC, Farkouh ME, Godoy LC, Lawler PR, Udell JA, Wijeysundera HC and Ko DT. Low-Density Lipoprotein Cholesterol and Adverse Cardiovascular Events After Percutaneous Coronary Intervention. *J Am Coll Cardiol*. 2020;76:1440-1450.
6. Violaris AG, Melkert R and Serruys PW. Influence of serum cholesterol and cholesterol subfractions on restenosis after successful coronary angioplasty. A quantitative angiographic analysis of 3336 lesions. *Circulation*. 1994;90:2267-79.
7. Catapano AL, Pirillo A and Norata GD. Vascular inflammation and low-density lipoproteins: is cholesterol the link? A lesson from the clinical trials. *Br J Pharmacol*. 2017;174:3973-3985. PMC5659993.
8. Collado A, Marques P, Domingo E, Perello E, González-Navarro H, Martinez-Hervás S, Real JT, Piqueras L, Ascaso JF and Sanz MJ. Novel Immune Features of the Systemic Inflammation Associated with Primary Hypercholesterolemia: Changes in Cytokine/Chemokine Profile, Increased Platelet and Leukocyte Activation. *J Clin Med*. 2018;8. PMC6352074.
9. Cybulsky MI, Iiyama K, Li H, Zhu S, Chen M, Iiyama M, Davis V, Gutierrez-Ramos JC, Connelly PW and Milstone DS. A major role for VCAM-1, but not ICAM-1, in early atherosclerosis. *J Clin Invest*. 2001;107:1255-62. PMC209298.
10. Gerhardt T and Ley K. Monocyte trafficking across the vessel wall. *Cardiovasc Res*. 2015;107:321-30. PMC4592323.
11. Libby P. Inflammation in atherosclerosis. *Arterioscler Thromb Vasc Biol*. 2012;32:2045-51. PMC3422754.
12. Chen JY, Ye ZX, Wang XF, Chang J, Yang MW, Zhong HH, Hong FF and Yang SL. Nitric oxide bioavailability dysfunction involves in atherosclerosis. *Biomed Pharmacother*. 2018;97:423-428.
13. Daub K, Seizer P, Stellos K, Krämer BF, Bigalke B, Schaller M, Fateh-Moghadam S, Gawaz M and Lindemann S. Oxidized LDL-activated platelets induce vascular inflammation. *Semin Thromb Hemost*. 2010;36:146-56.
14. Gąsecka A, Rogula S, Szarpak Ł and Filipiak KJ. LDL-Cholesterol and Platelets: Insights into Their Interactions in Atherosclerosis. *Life (Basel)*. 2021;11. PMC7826814.
15. Brown EJ and Frazier WA. Integrin-associated protein (CD47) and its ligands. *Trends Cell Biol*. 2001;11:130-5.
16. Isenberg JS, Roberts DD and Frazier WA. CD47: a new target in cardiovascular therapy. *Arterioscler Thromb Vasc Biol*. 2008;28:615-21. PMC2553319.

17. Finley MJ, Clark KA, Alferiev IS, Levy RJ and Stachelek SJ. Intracellular signaling mechanisms associated with CD47 modified surfaces. *Biomaterials*. 2013;34:8640-9. PMC3804223.
18. Stachelek SJ, Finley MJ, Alferiev IS, Wang F, Tsai RK, Eckells EC, Tomczyk N, Connolly JM, Discher DE, Eckmann DM and Levy RJ. The effect of CD47 modified polymer surfaces on inflammatory cell attachment and activation. *Biomaterials*. 2011;32:4317-26. PMC3108143.
19. Inamdar VV, Fitzpatrick E, Alferiev I, Nagaswami C, Spruce LA, Fazelinia H, Bratinov G, Seeholzer SH, Levy RJ, Fishbein I and Stachelek SJ. Stability and bioactivity of pepCD47 attachment on stainless steel surfaces. *Acta Biomater*. 2020;104:231-240. PMC7295035.
20. Slee JB, Alferiev IS, Nagaswami C, Weisel JW, Levy RJ, Fishbein I and Stachelek SJ. Enhanced biocompatibility of CD47-functionalized vascular stents. *Biomaterials*. 2016;87:82-92. PMC5304342.

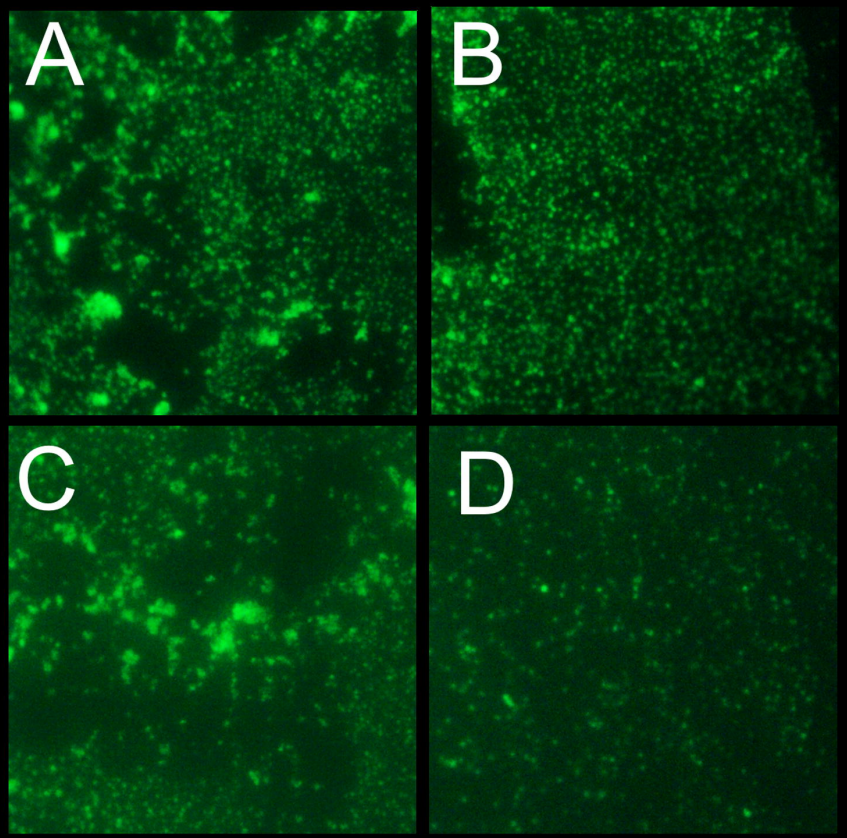
A
B
C
D

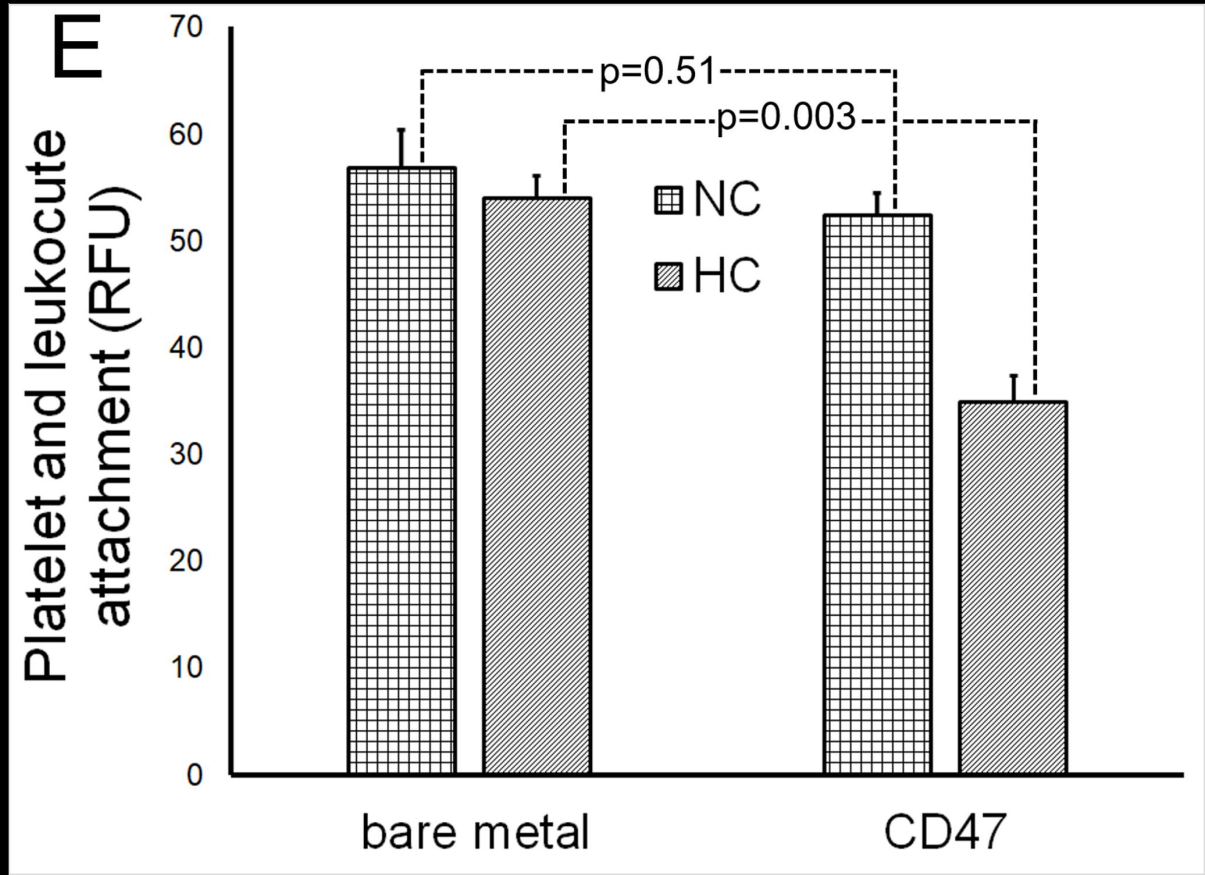
E
Platelet and leukocute attachment (RFU)
70
60
50
40
30
20
10
0
p=0.51
p=0.003
NC
HC
bare metal
CD47

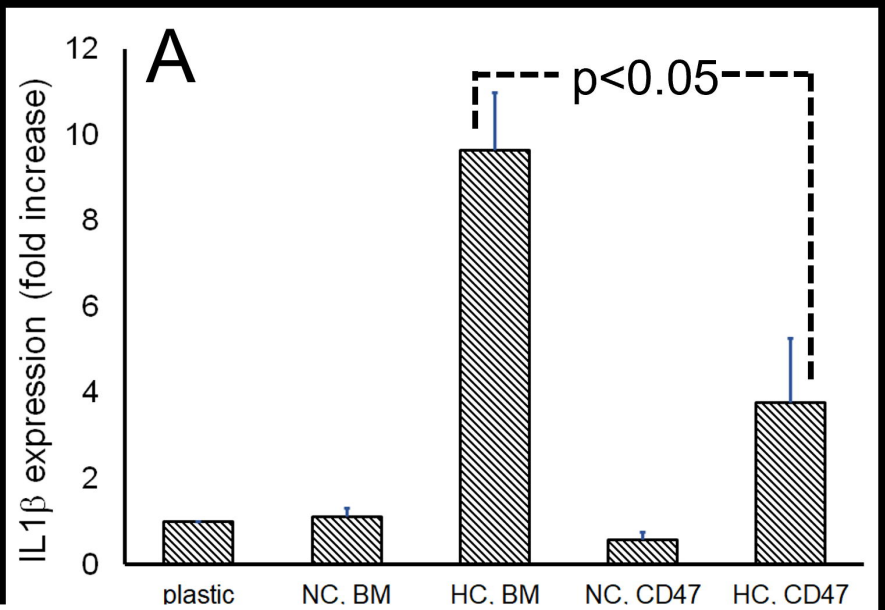
A
p<0.05
IL1β expression (fold increase)
0
2
4
6
8
10
12
plastic
NC. BM
HC. BM
NC. CD47
HC. CD47

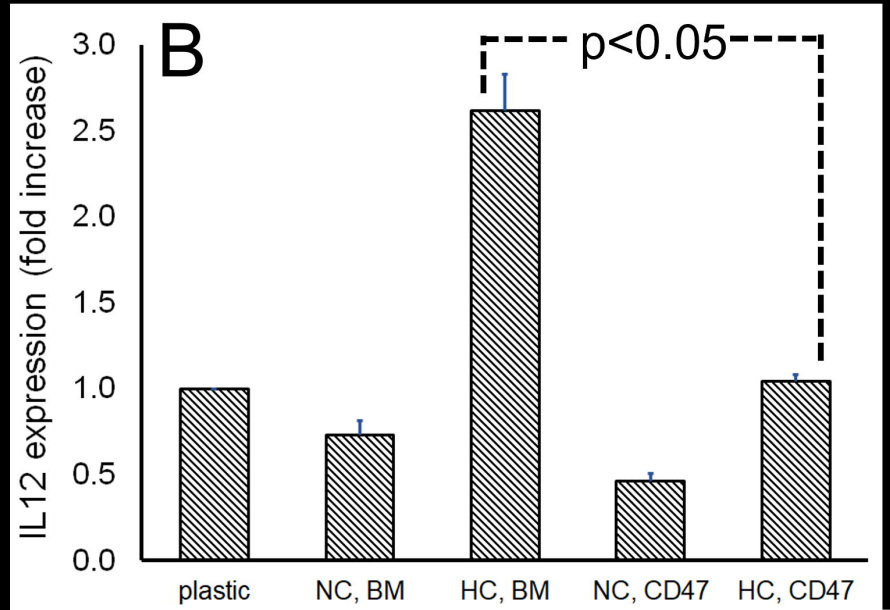
B
p<0.05
IL12 expression (fold increase)
0.0
0.5
1.0
1.5
2.0
2.5
3.0
plastic
NC, BM
HC, BM
NC, CD47
HC, CD47

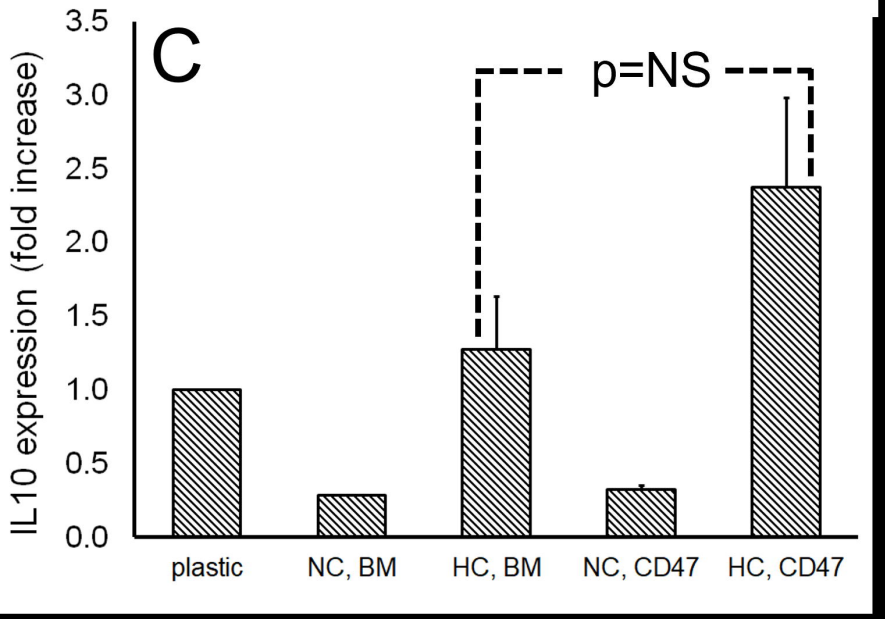
C
p=NS
IL10 expression (fold increase)
0.0
0.5
1.0
1.5
2.0
2.5
3.0
3.5
plastic
NC, BM
HC, BM
NC, CD47
HC, CD47

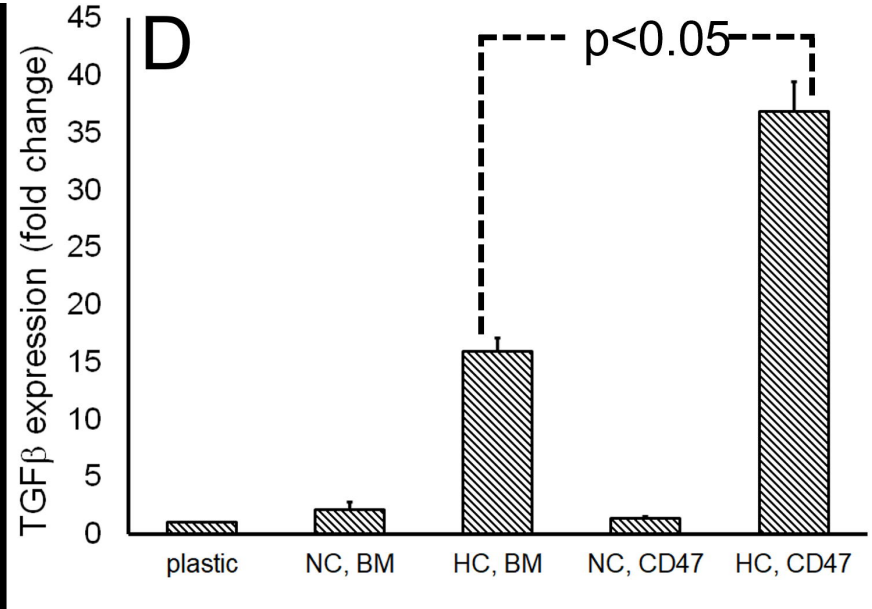
D
p<0.05
TGFβ expression (fold change)
0
5
10
15
20
25
30
35
40
45
plastic
NC, BM
HC, BM
NC, CD47
HC, CD47

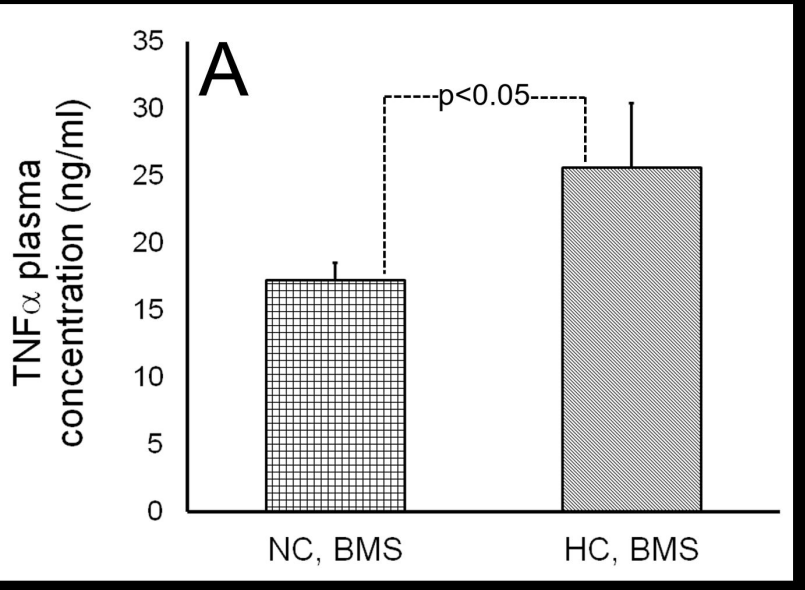
A
TNFα plasma concentration (ng/ml)
35
30
25
20
15
10
5
0
p<0.05
NC, BMS
HC, BMS

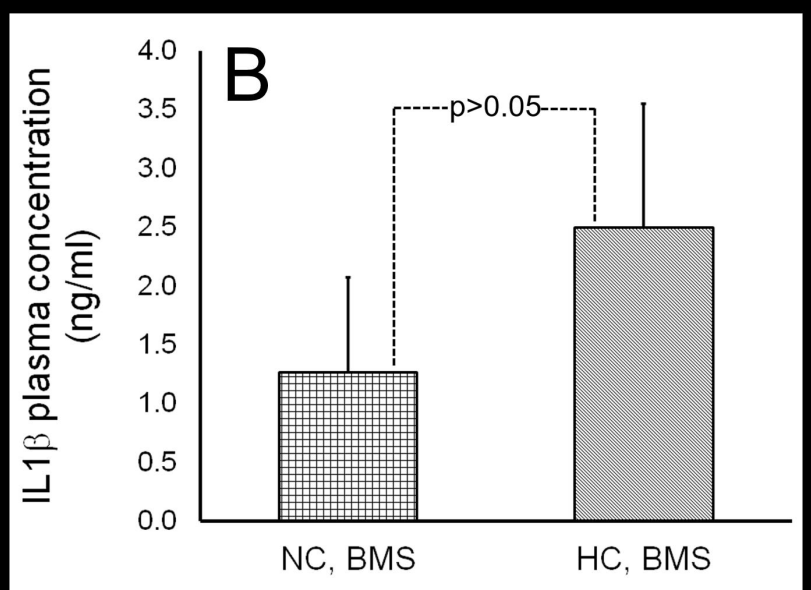
B
IL1β plasma concentration (ng/ml)
4.0
3.5
3.0
2.5
2.0
1.5
1.0
0.5
0.0
p>0.05
NC, BMS
HC, BMS

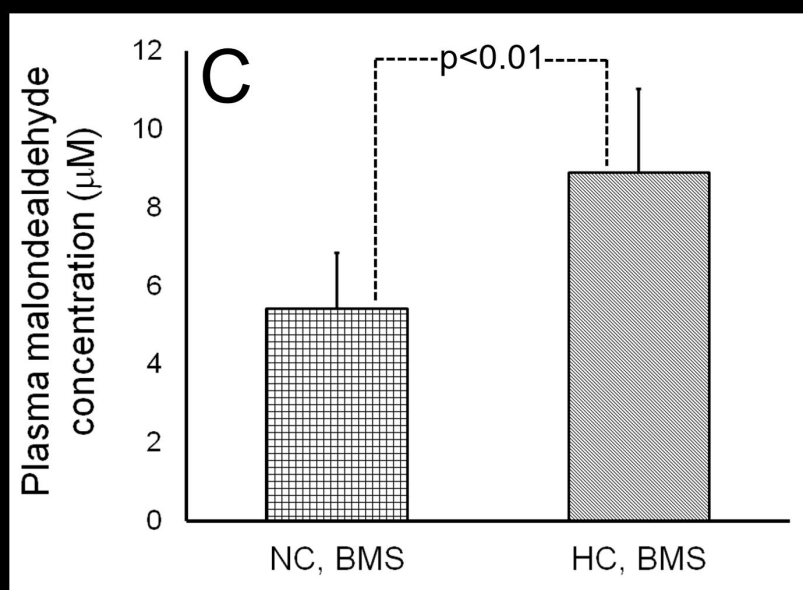
C
Plasma malondealdehyde concentration (μM)
12
10
8
6
4
2
0
p<0.01
NC, BMS
HC, BMS

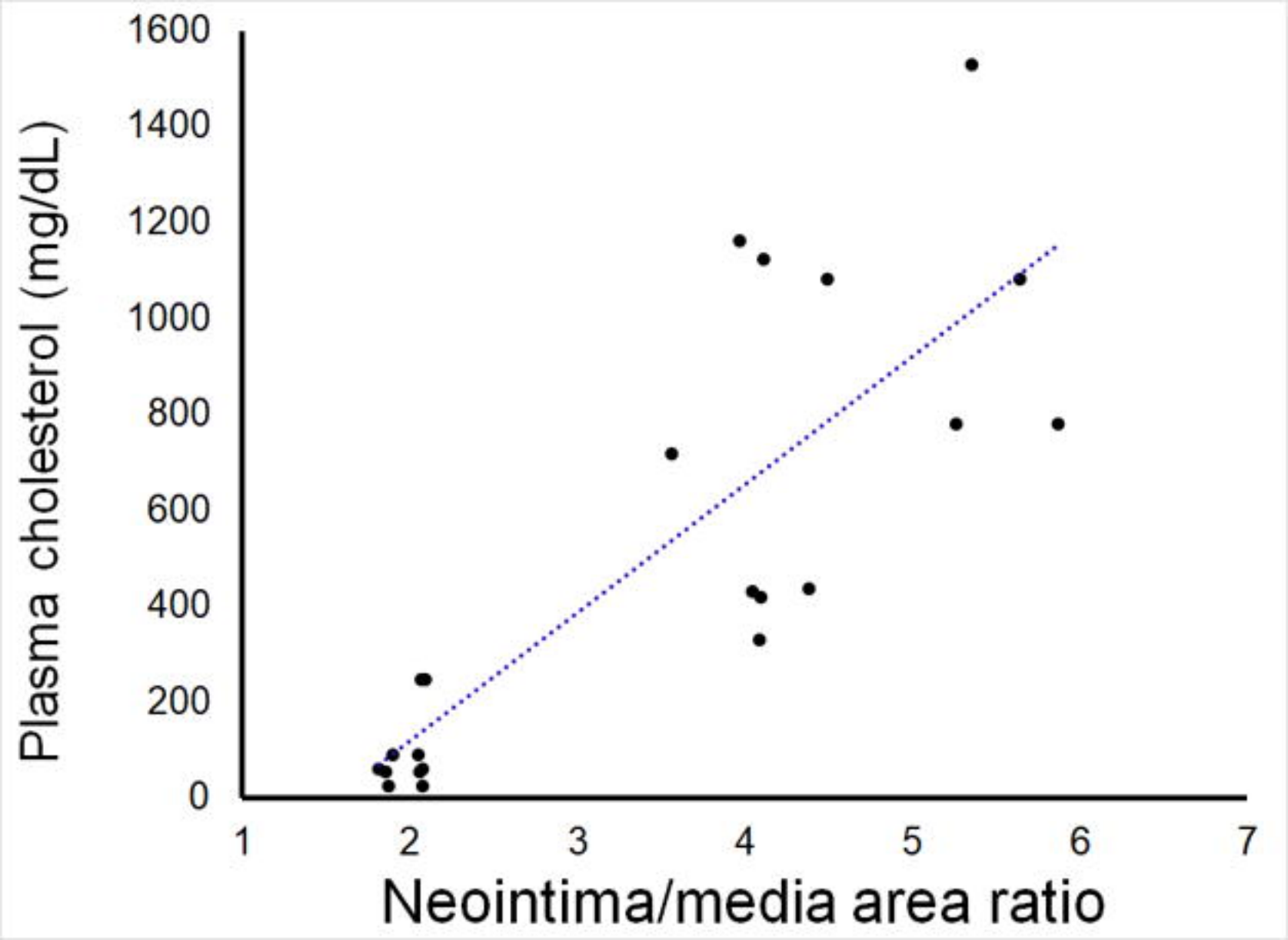
Plasma cholesterol (mg/dL)
1600
1400
1200
1000
800
600
400
200
0
1
2
3
4
5
6
7
Neointima/media area ratio

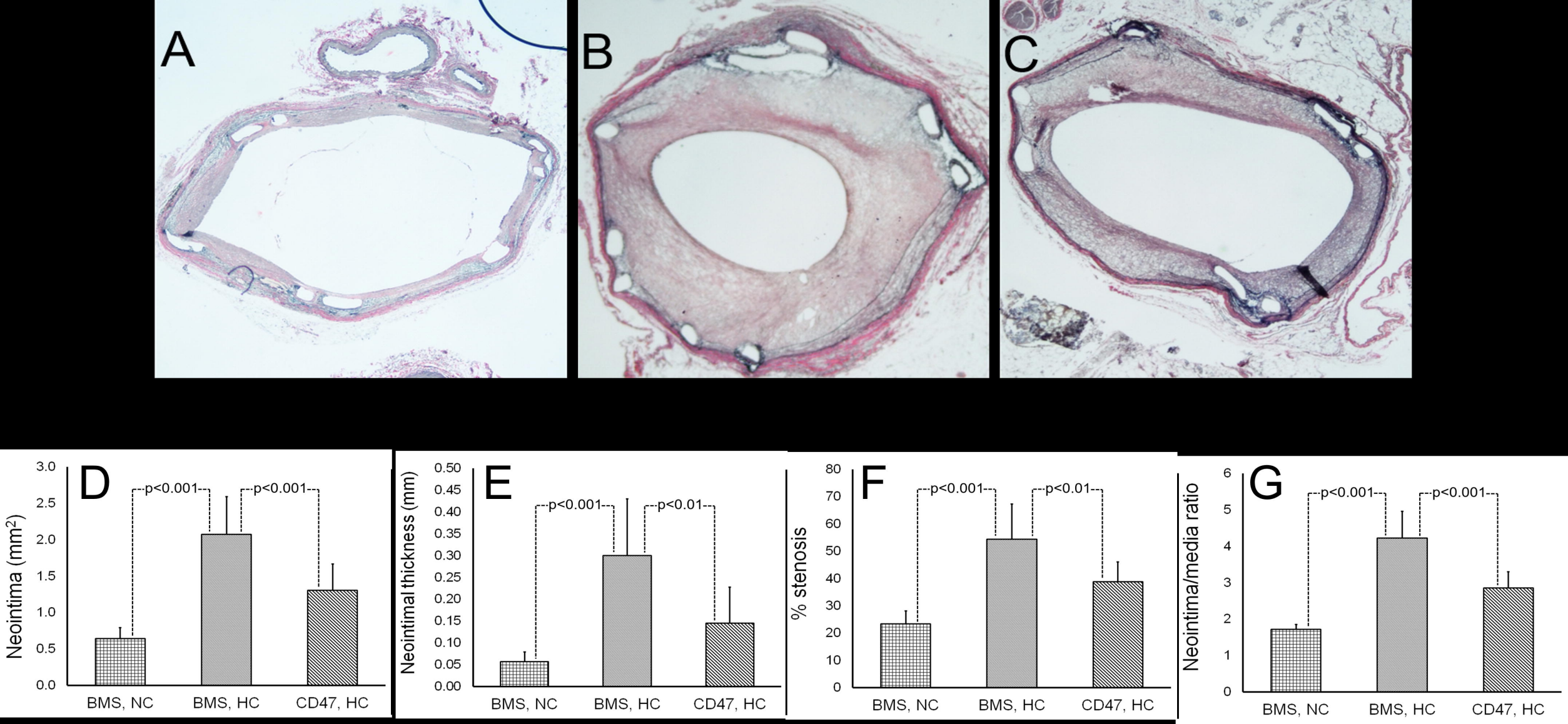
A
B
C
D
Neointima (mm²)
3.0
2.5
2.0
1.5
1.0
0.5
0.0
p<0.001
p<0.001
BMS, NC
BMS, HC
CD47, HC
E
Neointimal thickness (mm)
0.50
0.45
0.40
0.35
0.30
0.25
0.20
0.15
0.10
0.05
0.00
p<0.001
p<0.01
BMS, NC
BMS, HC
CD47, HC
F
% stenosis
80
70
60
50
40
30
20
10
0
p<0.001
p<0.01
BMS, NC
BMS, HC
CD47, HC
G
Neointima/media ratio
6
5
4
3
2
1
0
p<0.001
p<0.001
BMS, NC
BMS, HC
CD47, HC

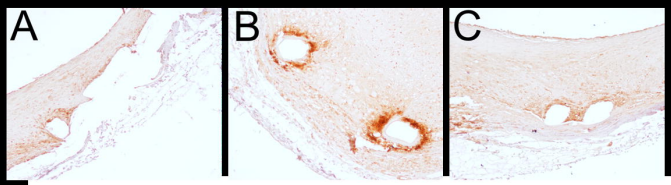
A
B
C

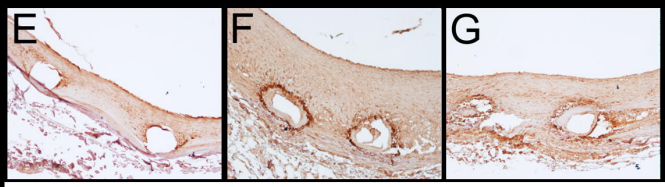
E
F
G

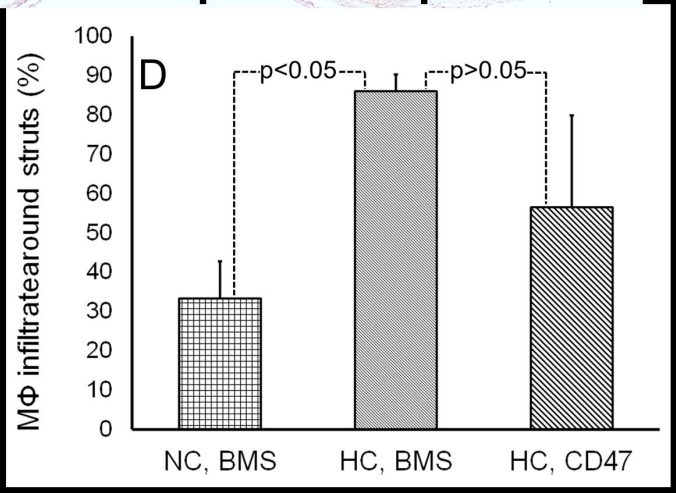
D
MΦ infiltratearound struts (%)
100
90
80
70
60
50
40
30
20
10
0
p<0.05
p>0.05
NC, BMS
HC, BMS
HC, CD47

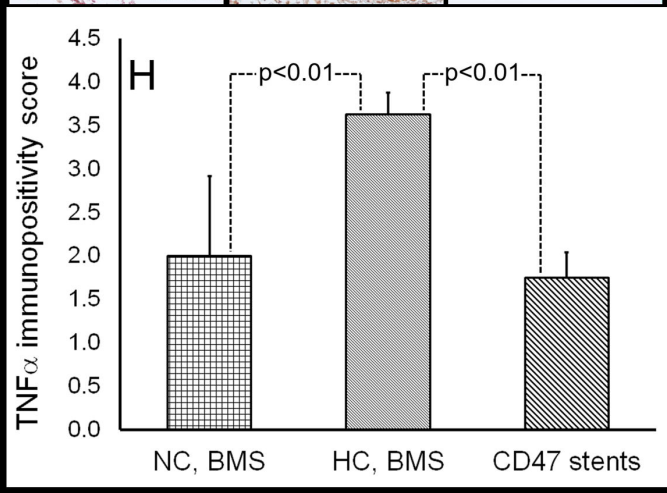
H
TNFα immunopositivity score
4.5
4.0
3.5
3.0
2.5
2.0
1.5
1.0
0.5
0.0
p<0.01
p<0.01
NC, BMS
HC, BMS
CD47 stents

I
J
K

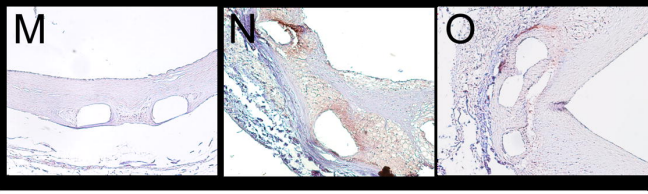
M
N
O

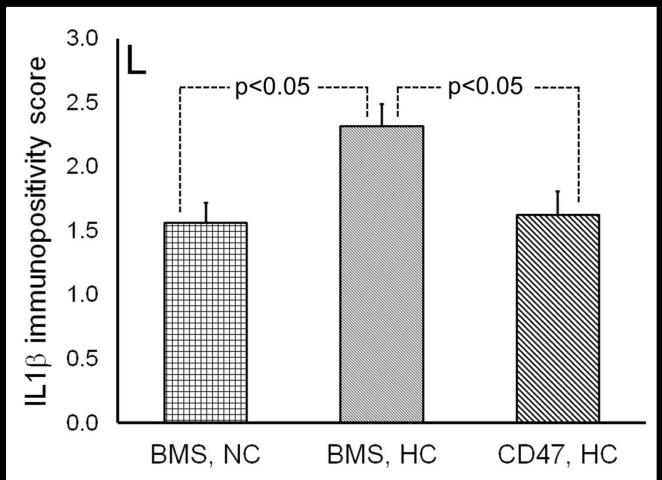
L
IL1β immunopositivity score
3.0
2.5
2.0
1.5
1.0
0.5
0.0
p<0.05
p<0.05
BMS, NC
BMS, HC
CD47, HC

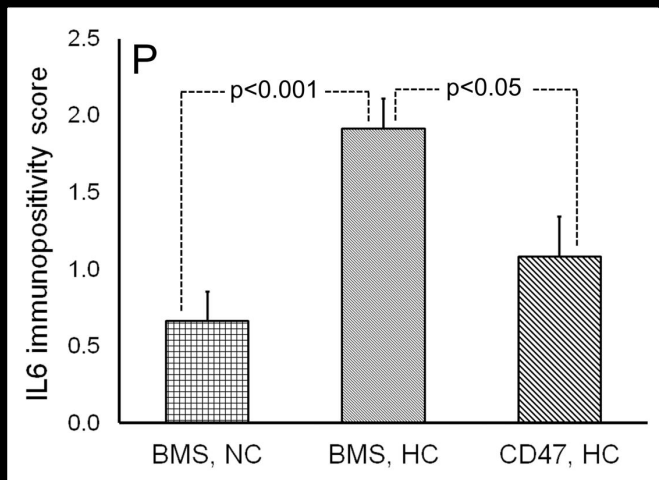
P
IL6 immunopositivity score
2.5
2.0
1.5
1.0
0.5
0.0
p<0.001
p<0.05
BMS, NC
BMS, HC
CD47, HC

CD 68

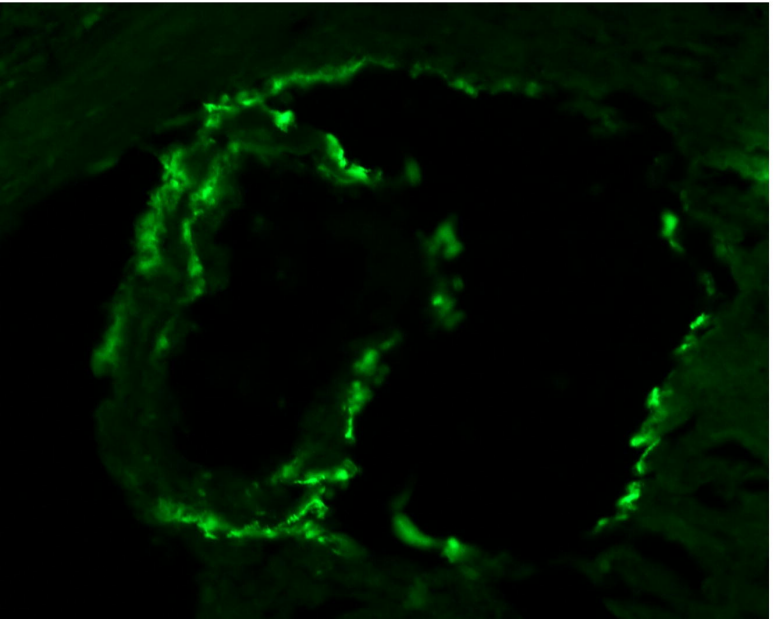

IL1β

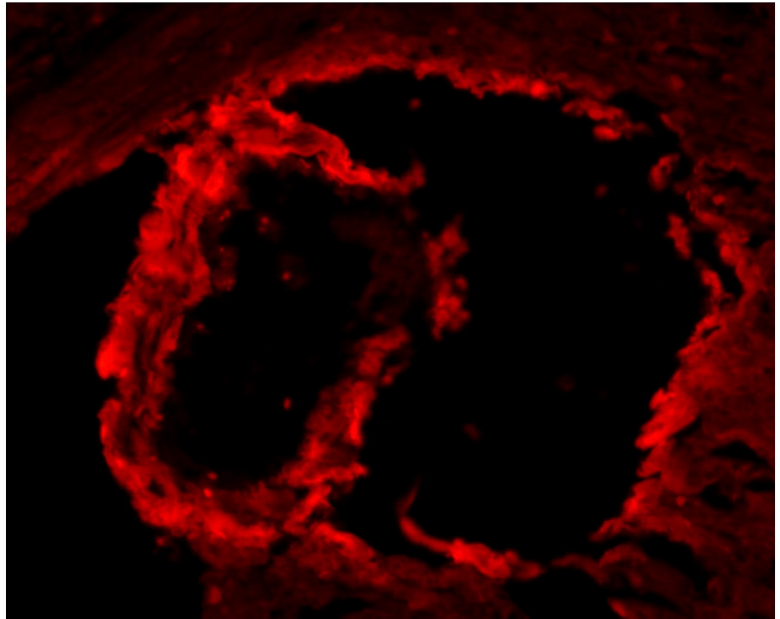

Merged

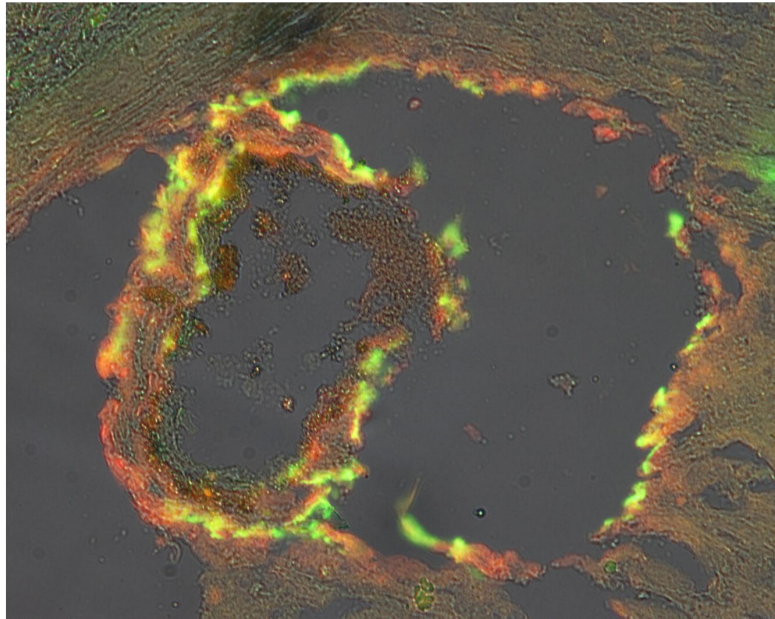

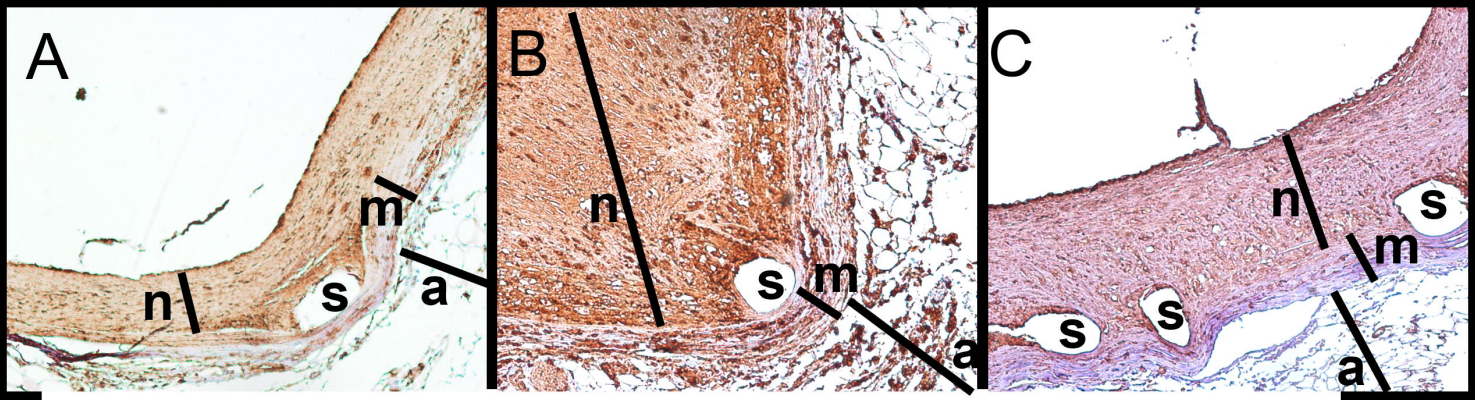
A
n
m
s
a
B
n
s
m
a
C
n
s
m
s
s
a

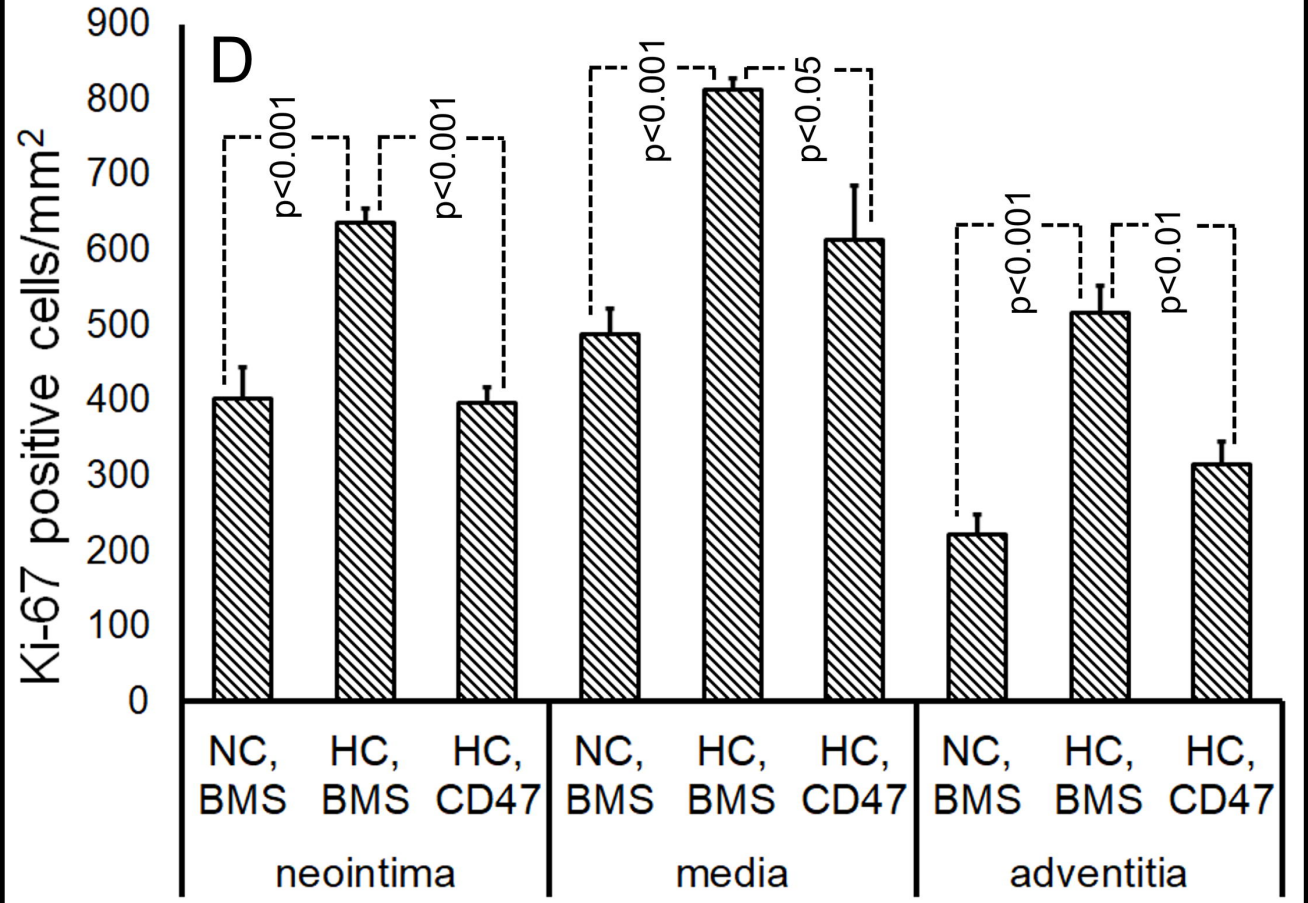
D
Ki-67 positive cells/mm2
900
800
700
600
500
400
300
200
100
0
p<0.001
p<0.001
p<0.001
p<0.05
p<0.001
p<0.01
NC, BMS
HC, BMS
HC, CD47
NC, BMS
HC, BMS
HC, CD47
NC, BMS
HC, BMS
HC, CD47
neointima
media
adventitia